Geometry and dynamics in moduli spaces

Lecture 3. Teichmüller Theorem. Square-tiled surfaces. Count of Masur–Veech volume through separatrix diagrams

Anton Zorich
Université Paris Cité

March 10, 2026

Teichmüller Theorem. Teichmüller geodesic flow

Flat metric associated to meromorphic quadratic differential

Construction 1. In a simply-connected coordinate chart $\mathcal{U}$, on a Riemann surface, in which a meromorphic quadratic differential $q(w) = \phi(w) \cdot (dw)^2$ does not have zeroes and poles, it can be represented as a square of a non-vanishing holomorphic 1-form: $q(w) = (\pm\omega(w))^2 = (\pm\sqrt{\phi(w)}dw)^2$. The form ω is defined up to a sign.

Flat metric associated to meromorphic quadratic differential

Construction 1. In a simply-connected coordinate chart $\mathcal{U}$, on a Riemann surface, in which a meromorphic quadratic differential $q(w) = \phi(w) \cdot (dw)^2$ does not have zeroes and poles, it can be represented as a square of a non-vanishing holomorphic 1-form: $q(w) = (\pm\omega(w))^2 = (\pm\sqrt{\phi(w)}dw)^2$.
The form ω is defined up to a sign.
We can choose a local coordinate z in $\mathcal{U}$ such that in this coordinate $\omega = dz$.
The coordinate $z = x + iy$ is defined up to an additive constant. It is called the *flat coordinate* associated to q. It defines a flat metric coming from the standard Euclidean plane endowed with coordinates x, y and *horizontal* ($y = const$) and *vertical* ($x = const$) foliations, which are orthogonal in our flat metric.
Neither the flat metric nor the foliations depend on a choice of sign of $\omega = dz$.

Flat metric associated to meromorphic quadratic differential

Construction 1. In a simply-connected coordinate chart $\mathcal{U}$, on a Riemann surface, in which a meromorphic quadratic differential $q(w) = \phi(w) \cdot (dw)^2$ does not have zeroes and poles, it can be represented as a square of a non-vanishing holomorphic 1-form: $q(w) = (\pm\omega(w))^2 = (\pm\sqrt{\phi(w)}dw)^2$.
The form ω is defined up to a sign.
We can choose a local coordinate z in $\mathcal{U}$ such that in this coordinate $\omega = dz$.
The coordinate $z = x + iy$ is defined up to an additive constant. It is called the *flat coordinate* associated to q. It defines a flat metric coming from the standard Euclidean plane endowed with coordinates x, y and *horizontal* ($y = const$) and *vertical* ($x = const$) foliations, which are orthogonal in our flat metric.
Neither the flat metric nor the foliations depend on a choice of sign of $\omega = dz$.

Construction 2. Let $w = u + iv$. Define a volume element in $\mathcal{U}$ as

$$-\frac{1}{2i}|\phi(w)|\, dw \wedge d\bar{w} = |\phi(w)|\, du \wedge dv$$

and a length element as $\sqrt{|\phi(w)|}\,|dw| = \sqrt{|\phi(w)|}\sqrt{du^2 + dv^2}$.

Exercise. Verify that the two constructions of the flat metric are equivalent and that the resulting metric does not depend on coordinates.

Half-translation surfaces

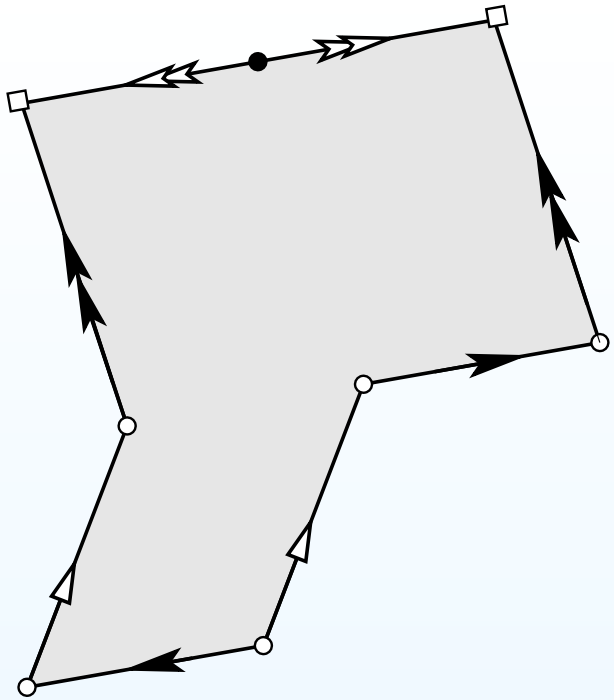

As in the case of Abelian differentials one can unwrap the resulting flat surface to a polygon. This time the sides are identified not only by parallel translations, but also by central symmetries. We still have distinguished vertical and horizontal directions. The difference with Abelian differentials is that now the holonomy group of the metric is $\mathbb{Z}/2\mathbb{Z}$: a parallel transport along a smooth loop can bring a tangent vector $\vec{v}$ back to itself or to $-\vec{v}$.

We can let the meromorphic quadratic differential have simple poles. They correspond to cone angles π of the metric. When the poles are at most simple, the area of the surface is still finite.

Coefficient of quasiconformality

Let X_1 and X_2 be Riemann surfaces of genus g. When complex structures are different there are no conformal maps from X_1 to X_2. A smooth map $f : X_1 \to X_2$ sends an infinitesimal circle at $x \in X_1$ to an infinitesimal ellipse at $f(x)$.

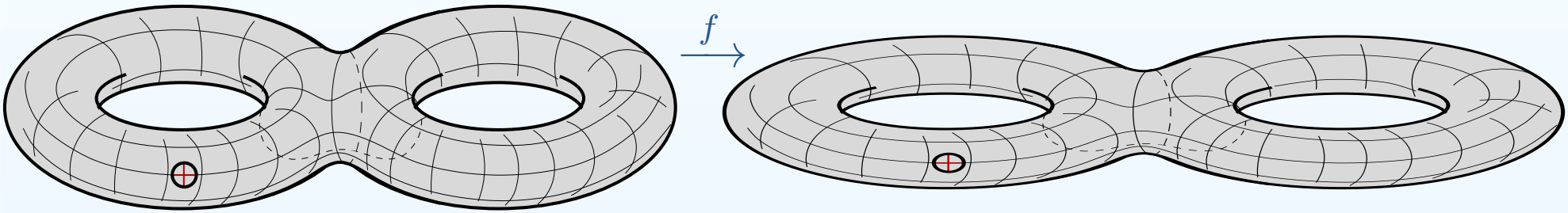

Coefficient of quasiconformality of f at $x \in X_1$ is the ratio $K_x(f) = \frac{a}{b}$ of demi-axis of this ellipse. *Coefficient of quasiconformality* of f is

$$K(f) = \sup_{x \in X_1} K_x(f).$$

Though X_1 is a compact Riemann surface we use $\sup$ and not $\max$ since the map f is allowed to have several isolated points x where the differential of f $D_x f : T_x X_1 \to T_{f(x)} X_2$ degenerates and where $K_x(f)$ is thus not defined.

Teichmüller Theorem

Theorem. *For any pair X_1, X_2 of Riemann surfaces of genus $g \geq 1$ there exist an extremal map $f_{ext} : X_1 \to X_2$ which minimizes the coefficient of quasiconformality $K(f)$. For this extremal map f_{ext} the coefficient of quasiconformality is constant everywhere on X_1 outside of a finite collection of points, where f_{ext} degenerates, and where $K_x(f_{ext})$ is not defined.*

Teichmüller Theorem

Theorem. *For any pair X_1, X_2 of Riemann surfaces of genus $g \geq 1$ there exist an extremal map $f_{ext} : X_1 \to X_2$ which minimizes the coefficient of quasiconformality $K(f)$. For this extremal map f_{ext} the coefficient of quasiconformality is constant everywhere on X_1 outside of a finite collection of points, where f_{ext} degenerates, and where $K_x(f_{ext})$ is not defined.*

One can choose a pair of holomorphic quadratic differentials q_1 on X_1 and q_2 on X_2, such that in the corresponding flat coordinates, the map f_{ext} acts as an expansion–contraction in respectively horizontal and vertical directions with a constant coefficient $\sqrt{K(f_{ext})}$. The foliations correspond to foliations of big (respectively small) demi-axes of ellipses.

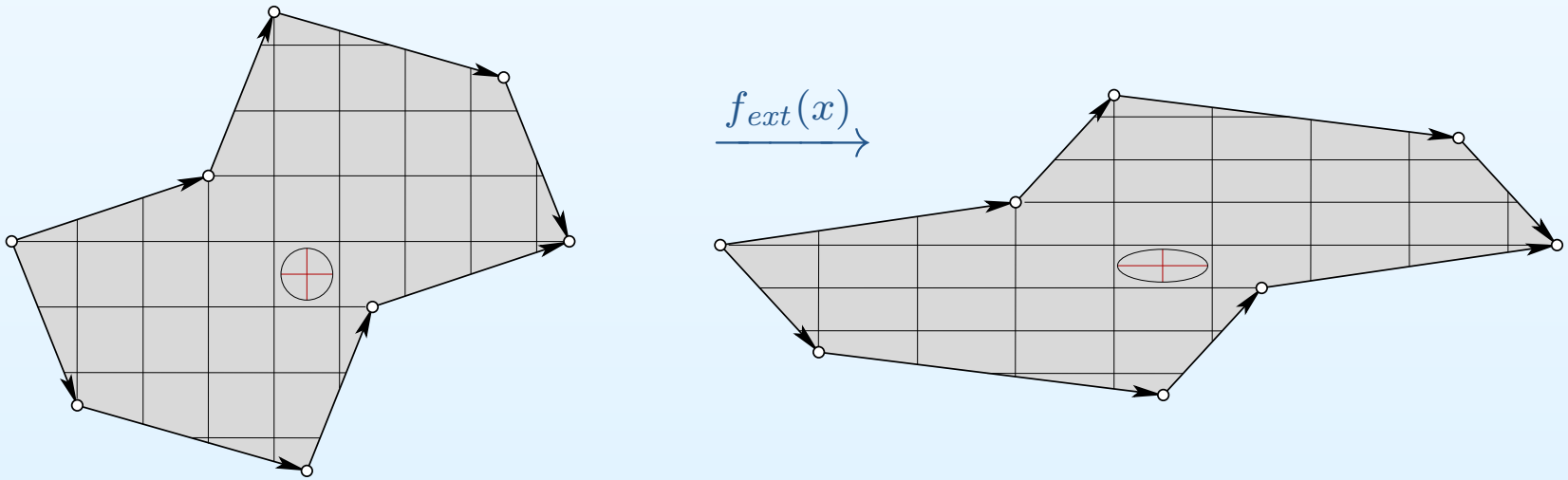

Teichmüller metric and Teichmüller geodesic flow.

Teichmüller metric measures the distance between two complex structures as

$$dist(X_1, X_2) = \frac{1}{2} \log K(f_{ext}),$$

where $f_{ext} : X_1 \to X_2$ is the extremal map. Any holomorphic quadratic differential defines a direction of deformation of the complex structure and a geodesic in the Teichmüller metric. Namely, a holomorphic quadratic differential defines a flat metric. A one-parameter family of maps, which in the flat coordinates are defined by diagonal matrices $g_t = \begin{pmatrix} e^t & 0 \\ 0 & e^{-t} \end{pmatrix}$, is a one-parameter family of extremal maps, so it forms a Teichmüller geodesic. According to the definition above we have $dist(X, g_t X) = t$.

Teichmüller metric and Teichmüller geodesic flow.

Teichmüller metric measures the distance between two complex structures as

$$dist(X_1, X_2) = \frac{1}{2} \log K(f_{ext}),$$

where $f_{ext} : X_1 \to X_2$ is the extremal map. Any holomorphic quadratic differential defines a direction of deformation of the complex structure and a geodesic in the Teichmüller metric. Namely, a holomorphic quadratic differential defines a flat metric. A one-parameter family of maps, which in the flat coordinates are defined by diagonal matrices $g_t = \begin{pmatrix} e^t & 0 \\ 0 & e^{-t} \end{pmatrix}$, is a one-parameter family of extremal maps, so it forms a Teichmüller geodesic. According to the definition above we have $dist(X, g_t X) = t$.

Remarks. The Teichmüller metric is not Riemannian but Finsler: it does not correspond to a quadratic form in the tangent space, but just to a norm which depends continuously on the point of the space of complex structures.

Teichmüller metric and Teichmüller geodesic flow.

Teichmüller metric measures the distance between two complex structures as

$$dist(X_1, X_2) = \frac{1}{2} \log K(f_{ext}),$$

where $f_{ext} : X_1 \to X_2$ is the extremal map. Any holomorphic quadratic differential defines a direction of deformation of the complex structure and a geodesic in the Teichmüller metric. Namely, a holomorphic quadratic differential defines a flat metric. A one-parameter family of maps, which in the flat coordinates are defined by diagonal matrices $g_t = \begin{pmatrix} e^t & 0 \\ 0 & e^{-t} \end{pmatrix}$, is a one-parameter family of extremal maps, so it forms a Teichmüller geodesic. According to the definition above we have $dist(X, g_t X) = t$.

Remarks. The Teichmüller metric is not Riemannian but Finsler: it does not correspond to a quadratic form in the tangent space, but just to a norm which depends continuously on the point of the space of complex structures.

Taking into consideration a functorial behavior of the vector bundle of holomorphic quadratic differentials, one can see, that it should be identified with a *cotangent* bundle (and not with a *tangent* bundle).

Square-tiled surfaces as integer points of the modular space

Counting volume by counting integer points in a large cone

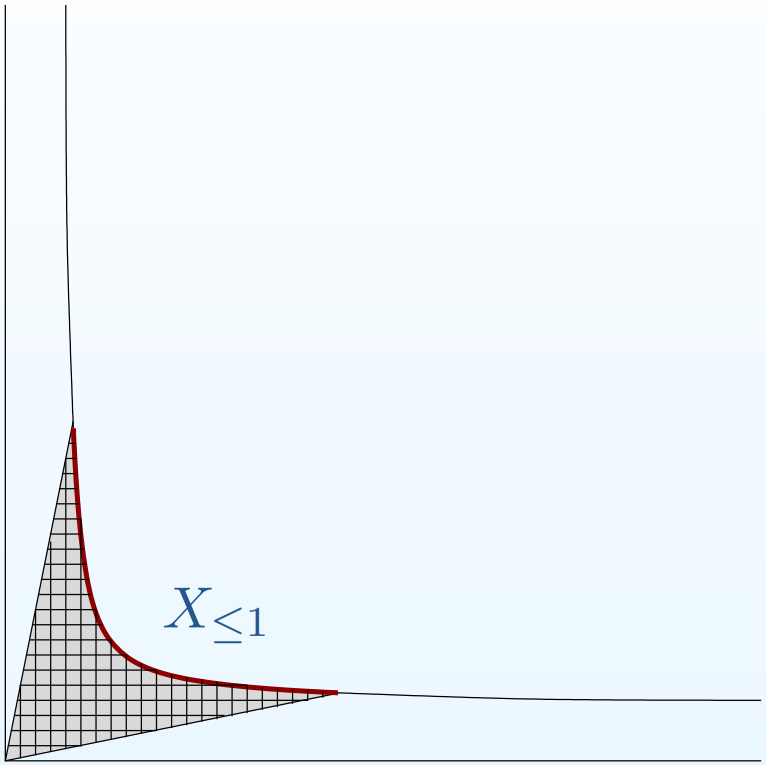

To count volume of the cone $X_{\leq 1}$ one can take an ε-grid and count the number of lattice points inside it.

Counting volume by counting integer points in a large cone

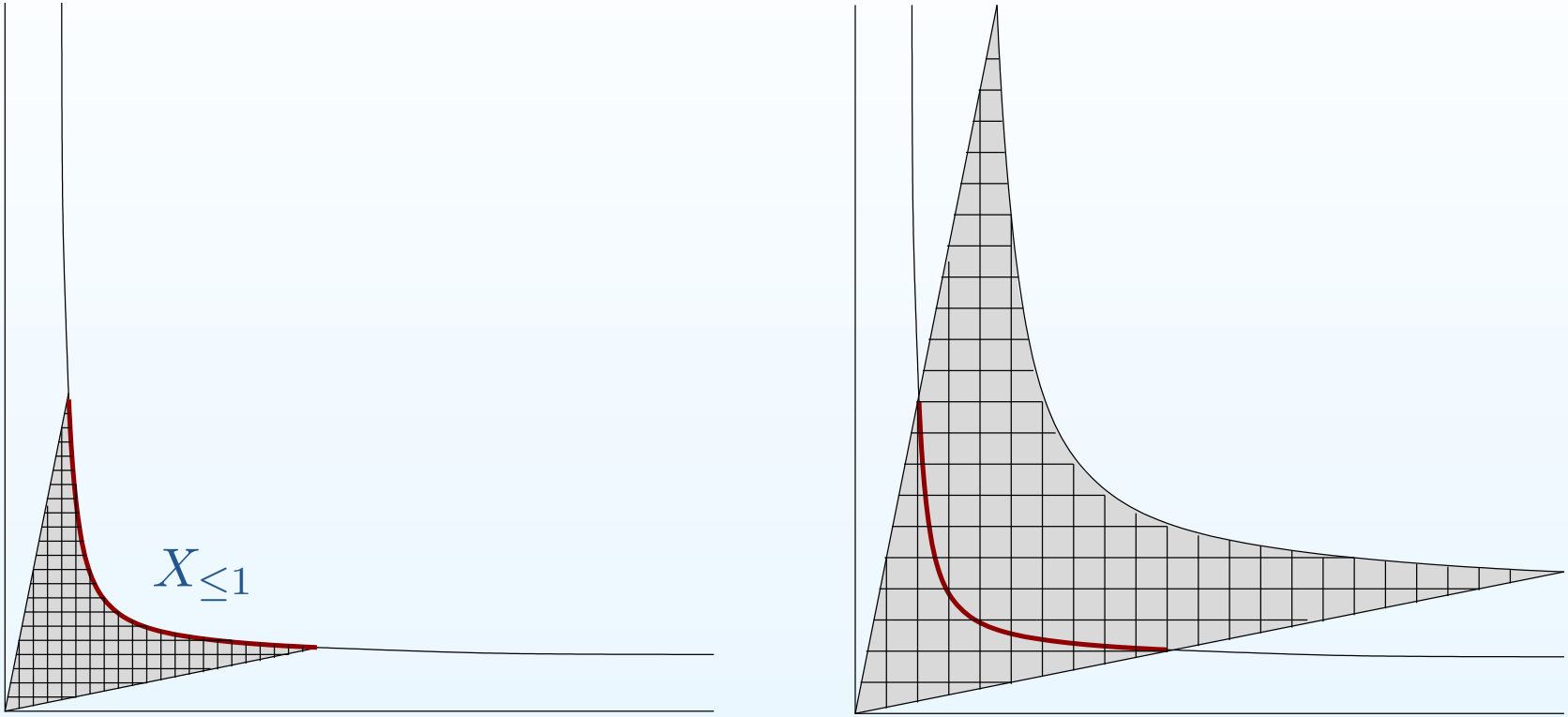

To count volume of the cone $X_{\leq 1}$ one can take an ε-grid and count the number of lattice points inside it.

Counting points of the ε-grid in the cone $X_{\leq 1}$ is the same as counting integer points in the proportionally rescaled cone $X_{\leq 1/\varepsilon}$.

Integer points as square-tiled surfaces

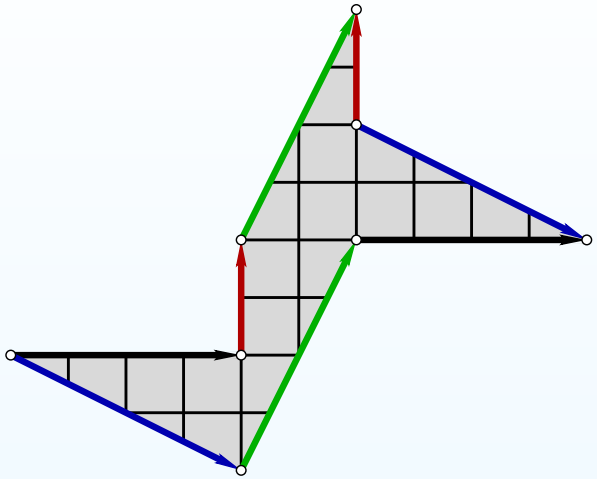

Integer points in period coordinates are represented by *square-tiled surfaces*.

Integer points as square-tiled surfaces

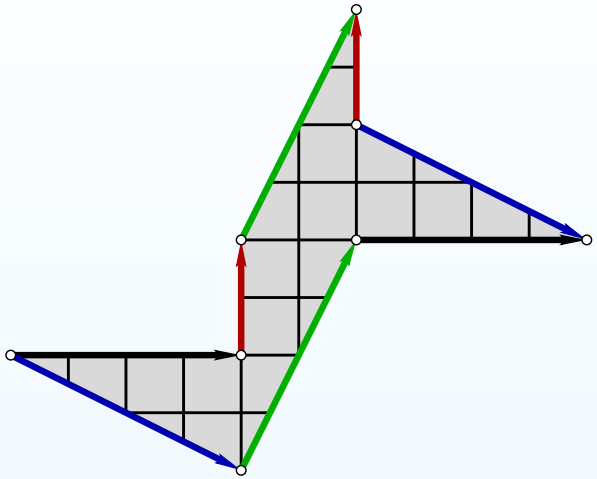

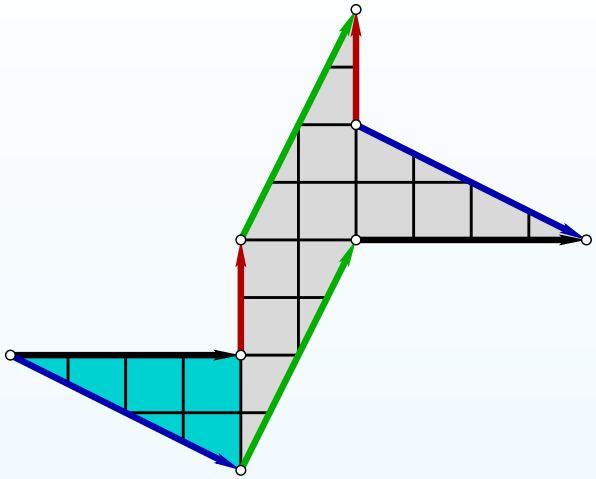

Integer points in period coordinates are represented by *square-tiled surfaces*.

Integer points as square-tiled surfaces

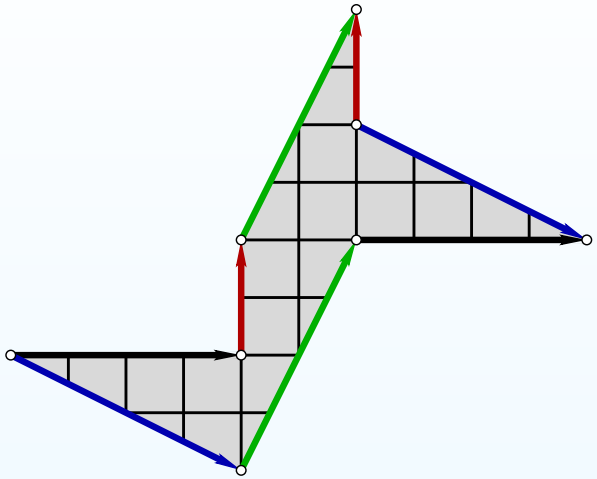

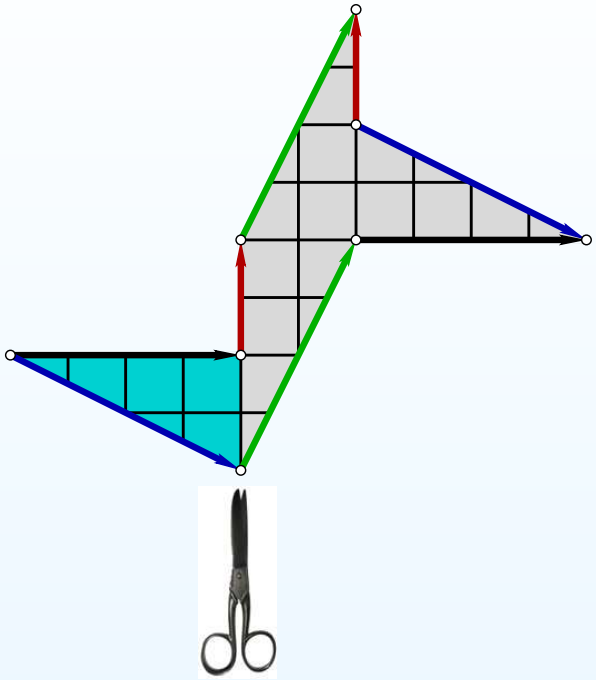

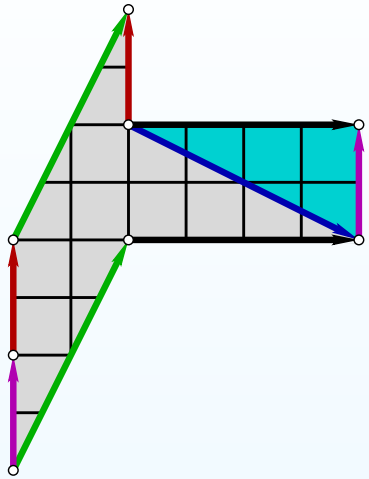

Integer points in period coordinates are represented by *square-tiled surfaces*.

Integer points as square-tiled surfaces

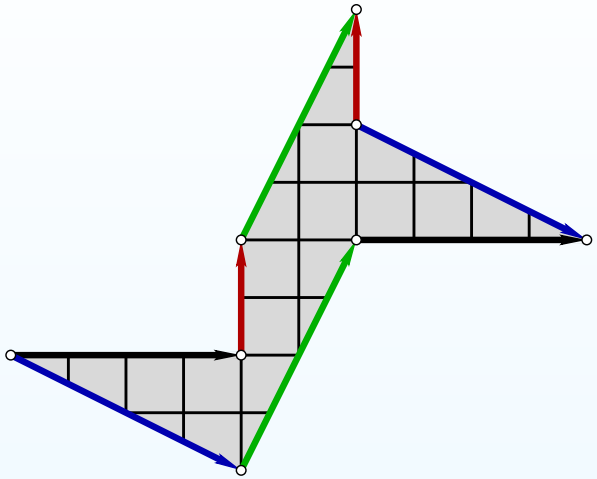

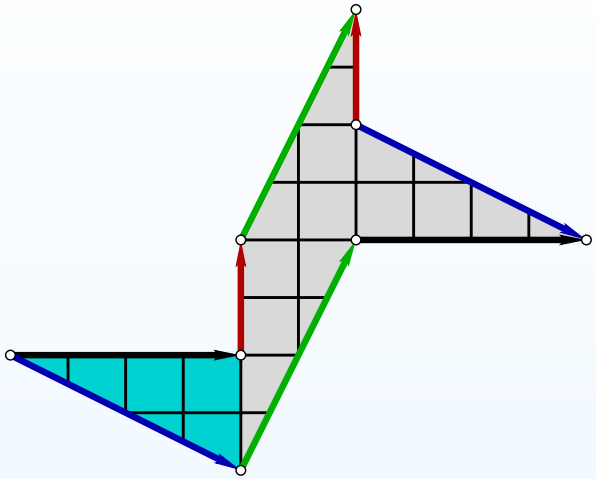

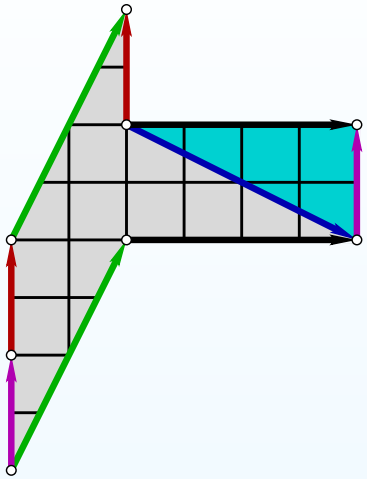

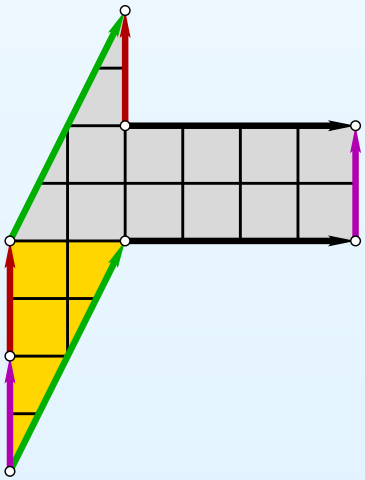

Integer points in period coordinates are represented by *square-tiled surfaces*.

Integer points as square-tiled surfaces

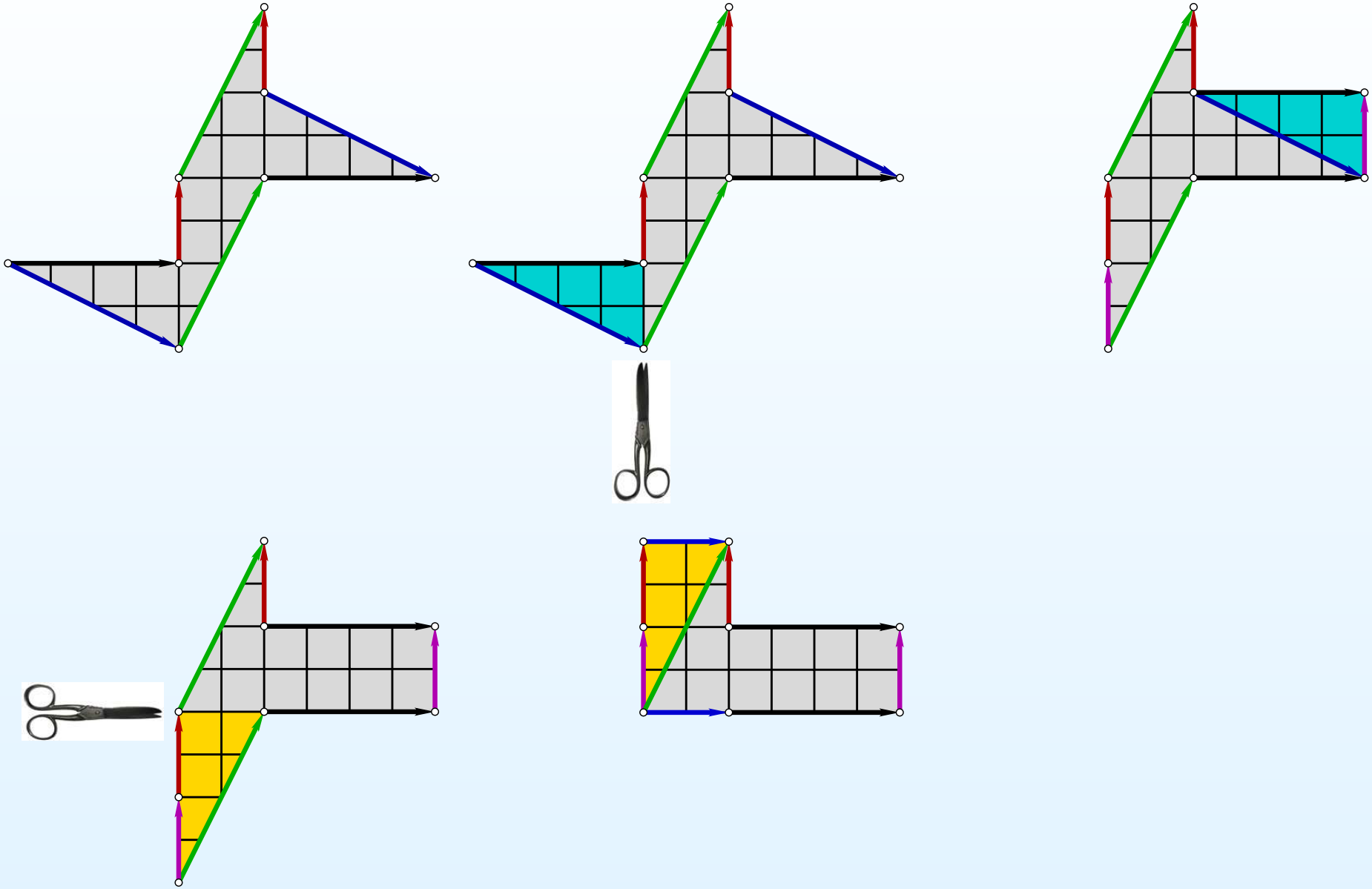

Integer points in period coordinates are represented by *square-tiled surfaces*.

Integer points as square-tiled surfaces

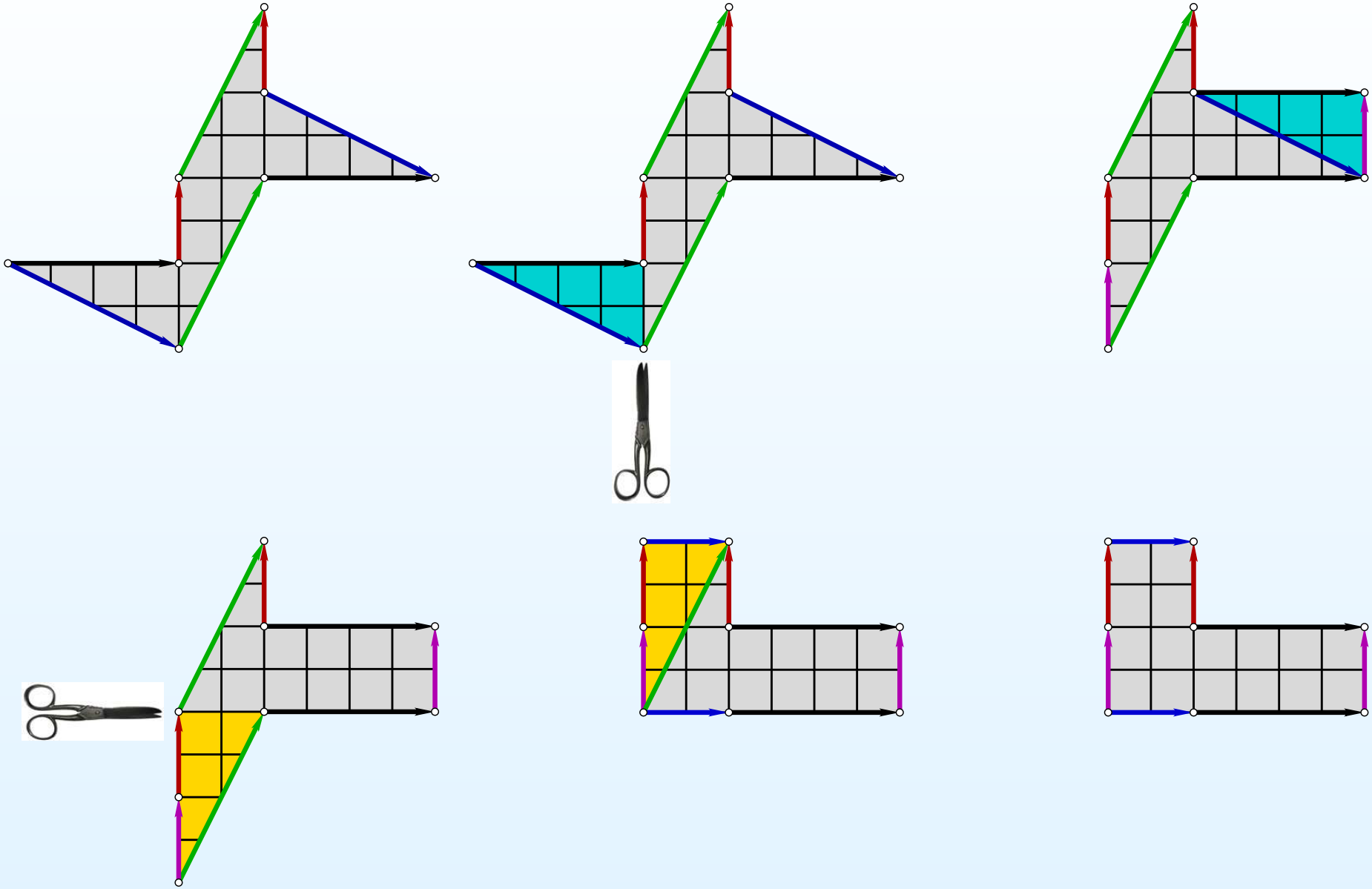

Integer points in period coordinates are represented by *square-tiled surfaces*.

Integer points as square-tiled surfaces

Integer points in period coordinates are represented by *square-tiled surfaces*. Indeed, if a flat surface S is defined by a holomorphic 1-form ω such that $[\omega] \in H^1(S, \{P_1, \ldots, P_n\}; \mathbb{Z} \oplus i\mathbb{Z})$, it has a canonical structure of a ramified cover p over the standard torus $\mathbb{T} = \mathbb{C}/(\mathbb{Z} \oplus i\mathbb{Z})$ ramified over a single point. Let P_1 be a zero of ω and $P \in C$ any point of the Riemann surface C. Define

$$\begin{array}{rccl} p: & P & \mapsto & \int_{P_1}^{P} \omega \ (\mathrm{mod}\ \mathbb{Z} \oplus i\mathbb{Z}) \\ p: & C & \to & \mathbb{T} = \mathbb{C}/(\mathbb{Z} \oplus i\mathbb{Z}) \end{array}$$

The ramification points of the cover p are exactly the zeroes of ω.

Integer points as square-tiled surfaces

Integer points in period coordinates are represented by *square-tiled surfaces*. Indeed, if a flat surface S is defined by a holomorphic 1-form ω such that $[\omega] \in H^1(S, \{P_1, \ldots, P_n\}; \mathbb{Z} \oplus i\mathbb{Z})$, it has a canonical structure of a ramified cover p over the standard torus $\mathbb{T} = \mathbb{C}/(\mathbb{Z} \oplus i\mathbb{Z})$ ramified over a single point. Let P_1 be a zero of ω and $P \in C$ any point of the Riemann surface C. Define

$$\begin{array}{rccl} p: & P & \mapsto & \int_{P_1}^{P} \omega \ (\mathrm{mod}\ \mathbb{Z} \oplus i\mathbb{Z}) \\ p: & C & \to & \mathbb{T} = \mathbb{C}/(\mathbb{Z} \oplus i\mathbb{Z}) \end{array}$$

The ramification points of the cover p are exactly the zeroes of ω.

Choosing the standard unit square pattern for $\mathbb{T}$ we get induced tiling of (C, ω) by unit squares which form horizontal and vertical cylinders. The square-tiled surface of genus two in the picture has 2 maximal horizontal cylinders filled with periodic geodesics.

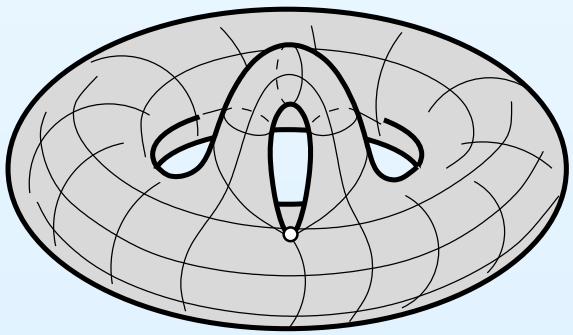

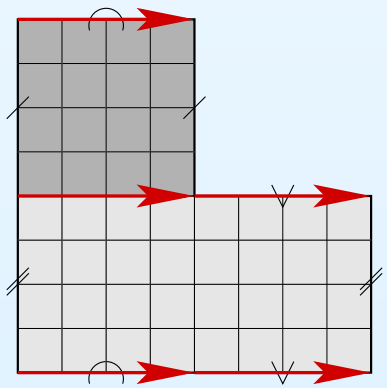

Masur–Veech volumes through count of square-tiled surfaces

Square-tiled surfaces which represent integer points in a "ball $\mathcal{H}_{area\leq N}$ of radius N" in a given stratum $\mathcal{H}$ of Abelian differentials are the ones, tiled with at most N unit squares. Denote the corresponding set by $\mathcal{ST}_N(\mathcal{H})$. We have,

$$\nu(\mathcal{H}_{area\leq N}) \sim \mathrm{card}(\mathcal{ST}_N(\mathcal{H}))\,.$$

By homogeneity of the Masur–Veech volume element ν we get

$$\nu(\mathcal{H}_{area\leq R}) = R^d \cdot \nu(\mathcal{H}_{area\leq 1})\,,$$

where

$$d = \dim_{\mathbb{C}} \mathcal{H}(m_1,\ldots,m_n) = 2g+n-1\,.$$

Thus,

$$\nu(\mathcal{H}_{\leq 1}) = \lim_{N\to+\infty} \frac{\mathrm{card}(\mathcal{ST}_N)}{N^d}\,.$$

By definition of the Masur–Veech volume $\mathrm{Vol}\,\mathcal{H}_1$ of the " unit sphere $\mathcal{H}_1 = \mathcal{H}_{area=1}$", we have $\mathrm{Vol}\,\mathcal{H}_1 = 2d\cdot\nu(\mathcal{H}_{area\leq 1})$. Combining, we get

$$\mathrm{Vol}\,\mathcal{H}_1(m_1,\ldots,m_n) := 2(2g+n-1)\cdot \lim_{N\to+\infty} \frac{\mathrm{card}(\mathcal{ST}_N(\mathcal{H}(m_1,\ldots,m_n)))}{N^d}\,.$$

Count of square-tiled surfaces

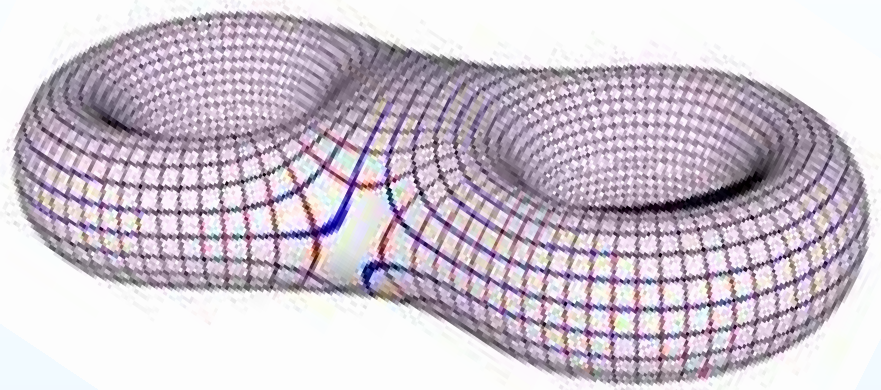

Picture created by Jian Jiang

We reduced evaluation of the Masur–Veech volumes $\operatorname{Vol}\mathcal{H}(m_1,\dots,m_n)$ to a combination of the following two related problems:

- Describe all combinatorial types of square-tiled surfaces in any given stratum $\mathcal{H}(m_1,\dots,m_n)$.
- Count the leading term in the asymptotics of the number of square-tiled surfaces of any given combinatorial type tiled with at most N squares when $N \to +\infty$.

Count of square-tiled surfaces through separatrix diagrams

Baby case: decomposition of a square-tiled torus

Let us count the number $\mathrm{card}(\mathcal{ST}_N(\mathcal{H}(0))$ of square-tiled tori tiled by at most $N \gg 1$ squares. Cutting a square-tiled torus by a horizontal waist curve we get a cylinder of integer height h. A waist curve of the cylinder has integer length w. The number of squares in the tiling equals $w \cdot h$.

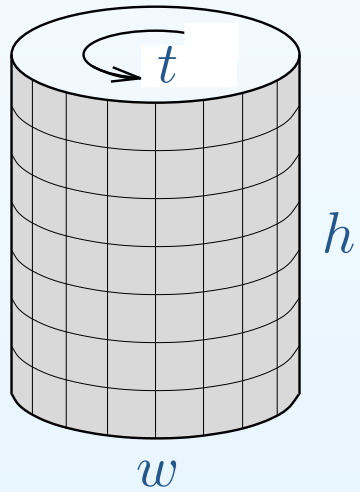

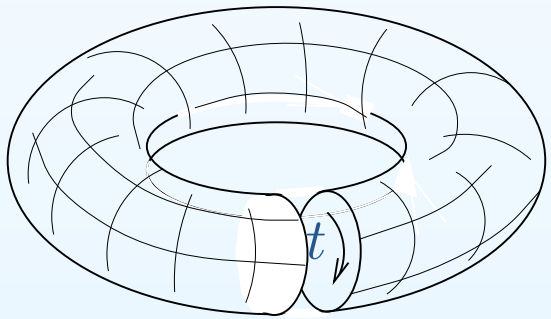

The way, in which two boundary components of the cylinder are identified, is described by an integer *twist* t which can take any value in $\{0, 1, \ldots, w-1\}$. Thus, for any fixed $w, h \in \mathbb{N}$ we get exactly w distinct square-tiled tori.

Baby case: counting square-tiled tori

We get the following leading term for $\mathrm{card}(\mathcal{ST}_N(\mathcal{H}(0))$ as $N \to +\infty$.

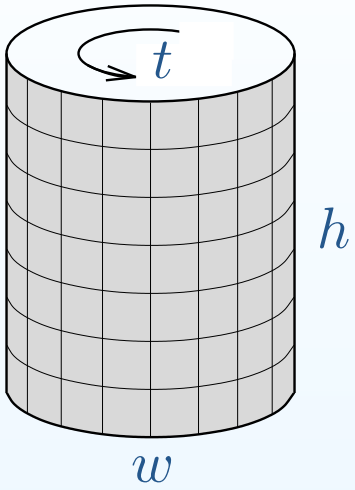

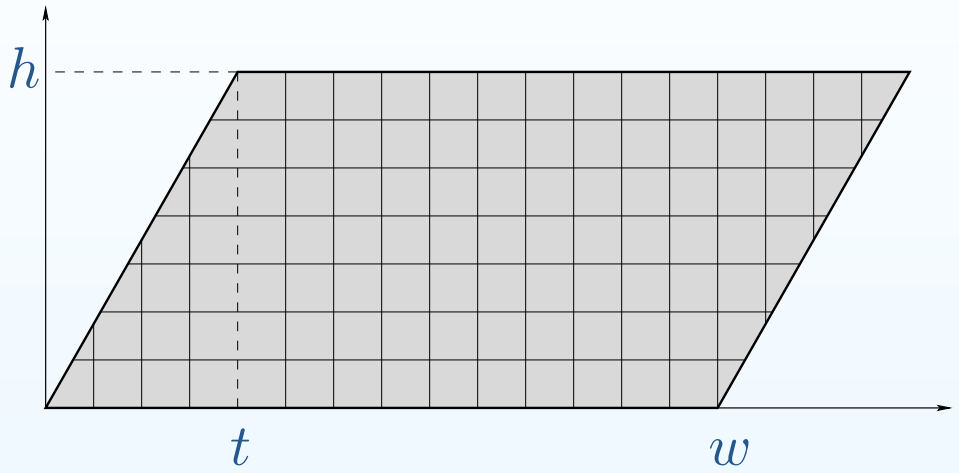

$$\mathrm{card}(\mathcal{ST}_N(\mathcal{H}(0)) = \sum_{\substack{w,h\in\mathbb{N}\\ w\cdot h\leq N}} w = \sum_{\substack{w,h\in\mathbb{N}\\ w\leq \frac{N}{h}}} w \sim \sum_{h\in\mathbb{N}} \frac{1}{2}\cdot\left(\frac{N}{h}\right)^2 = \frac{N^2}{2}\sum_{h\in\mathbb{N}}\frac{1}{h^2}$$

$$= \frac{N^2}{2}\cdot\zeta(2) = \frac{N^2}{2}\cdot\frac{\pi^2}{6}.$$

Our formula gives

$$\mathrm{Vol}\,\mathcal{H}_1(0) := 2d\cdot\lim_{N\to+\infty}\frac{\mathrm{card}(\mathcal{ST}_N(\mathcal{H}(0)))}{N^d} = \frac{\pi^2}{3}.$$

Critical graph (separatrix diagram)

Note that all leaves of the horizontal (vertical) foliation on a square-tiled surface are closed. The *critical graph* Γ (*separatrix diagram*) is the union of all horizontal critical leaves. Vertices of Γ are represented by the conical points; the edges of Γ are formed by horizontal saddle connections (red in the picture).

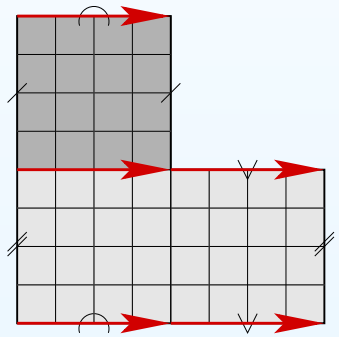

Critical graph (separatrix diagram)

Note that all leaves of the horizontal (vertical) foliation on a square-tiled surface are closed. The *critical graph* Γ (*separatrix diagram*) is the union of all horizontal critical leaves. Vertices of Γ are represented by the conical points; the edges of Γ are formed by horizontal saddle connections (red in the picture).

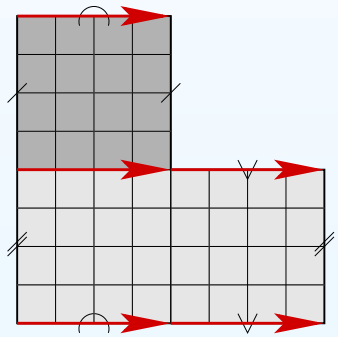

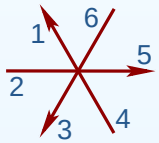

Let us construct the critical graph step-by-step. In our example the cone angle is 6π, so there are three outgoing separatrix rays and three incoming rays; they are alternated with respect to the natural cyclic order.

Critical graph (separatrix diagram)

Note that all leaves of the horizontal (vertical) foliation on a square-tiled surface are closed. The *critical graph* Γ (*separatrix diagram*) is the union of all horizontal critical leaves. Vertices of Γ are represented by the conical points; the edges of Γ are formed by horizontal saddle connections (red in the picture).

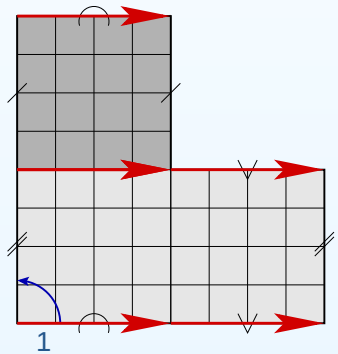

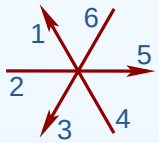

Let us construct the critical graph step-by-step. In our example the cone angle is 6π, so there are three outgoing separatrix rays and three incoming rays; they are alternated with respect to the natural cyclic order. Going around our conical singularity we can trace the order of appearance of horizontal rays and the way the prongs are joined into a graph.

Critical graph (separatrix diagram)

Note that all leaves of the horizontal (vertical) foliation on a square-tiled surface are closed. The *critical graph* Γ (*separatrix diagram*) is the union of all horizontal critical leaves. Vertices of Γ are represented by the conical points; the edges of Γ are formed by horizontal saddle connections (red in the picture).

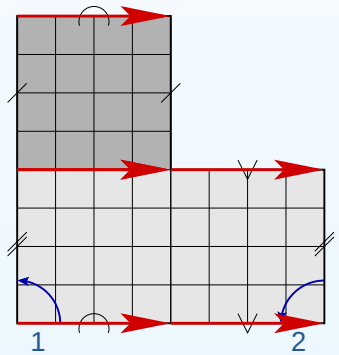

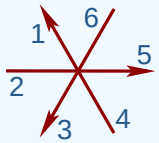

Let us construct the critical graph step-by-step. In our example the cone angle is 6π, so there are three outgoing separatrix rays and three incoming rays; they are alternated with respect to the natural cyclic order. Going around our conical singularity we can trace the order of appearance of horizontal rays and the way the prongs are joined into a graph.

Critical graph (separatrix diagram)

Note that all leaves of the horizontal (vertical) foliation on a square-tiled surface are closed. The *critical graph* Γ (*separatrix diagram*) is the union of all horizontal critical leaves. Vertices of Γ are represented by the conical points; the edges of Γ are formed by horizontal saddle connections (red in the picture).

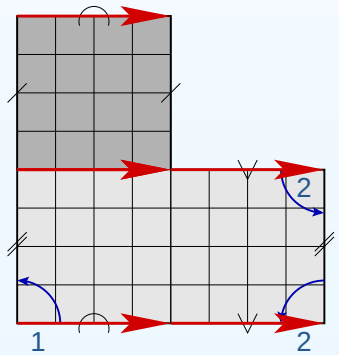

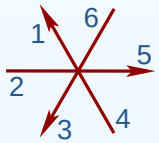

Let us construct the critical graph step-by-step. In our example the cone angle is 6π, so there are three outgoing separatrix rays and three incoming rays; they are alternated with respect to the natural cyclic order. Going around our conical singularity we can trace the order of appearance of horizontal rays and the way the prongs are joined into a graph.

Critical graph (separatrix diagram)

Note that all leaves of the horizontal (vertical) foliation on a square-tiled surface are closed. The *critical graph* Γ (*separatrix diagram*) is the union of all horizontal critical leaves. Vertices of Γ are represented by the conical points; the edges of Γ are formed by horizontal saddle connections (red in the picture).

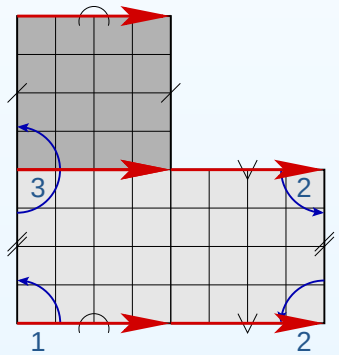

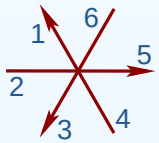

Let us construct the critical graph step-by-step. In our example the cone angle is 6π, so there are three outgoing separatrix rays and three incoming rays; they are alternated with respect to the natural cyclic order. Going around our conical singularity we can trace the order of appearance of horizontal rays and the way the prongs are joined into a graph.

Critical graph (separatrix diagram)

Note that all leaves of the horizontal (vertical) foliation on a square-tiled surface are closed. The *critical graph* Γ (*separatrix diagram*) is the union of all horizontal critical leaves. Vertices of Γ are represented by the conical points; the edges of Γ are formed by horizontal saddle connections (red in the picture).

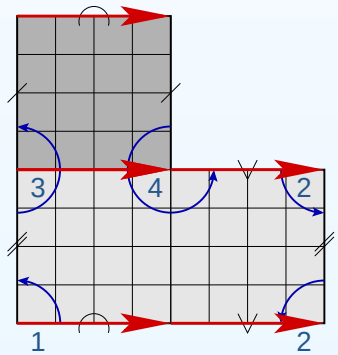

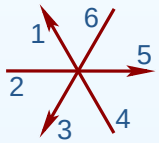

Let us construct the critical graph step-by-step. In our example the cone angle is 6π, so there are three outgoing separatrix rays and three incoming rays; they are alternated with respect to the natural cyclic order. Going around our conical singularity we can trace the order of appearance of horizontal rays and the way the prongs are joined into a graph.

Critical graph (separatrix diagram)

Note that all leaves of the horizontal (vertical) foliation on a square-tiled surface are closed. The *critical graph* Γ (*separatrix diagram*) is the union of all horizontal critical leaves. Vertices of Γ are represented by the conical points; the edges of Γ are formed by horizontal saddle connections (red in the picture).

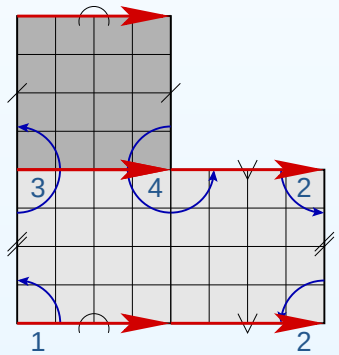

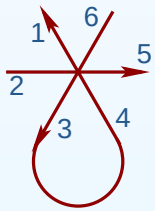

Let us construct the critical graph step-by-step. In our example the cone angle is 6π, so there are three outgoing separatrix rays and three incoming rays; they are alternated with respect to the natural cyclic order. Going around our conical singularity we can trace the order of appearance of horizontal rays and the way the prongs are joined into a graph. We see that the prong 3 is joined to prong 4;

Critical graph (separatrix diagram)

Note that all leaves of the horizontal (vertical) foliation on a square-tiled surface are closed. The *critical graph* Γ (*separatrix diagram*) is the union of all horizontal critical leaves. Vertices of Γ are represented by the conical points; the edges of Γ are formed by horizontal saddle connections (red in the picture).

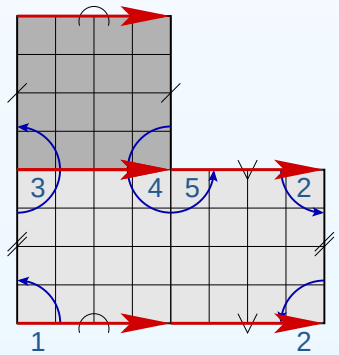

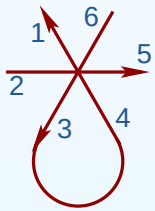

Let us construct the critical graph step-by-step. In our example the cone angle is 6π, so there are three outgoing separatrix rays and three incoming rays; they are alternated with respect to the natural cyclic order. Going around our conical singularity we can trace the order of appearance of horizontal rays and the way the prongs are joined into a graph. We see that the prong 3 is joined to prong 4;

Critical graph (separatrix diagram)

Note that all leaves of the horizontal (vertical) foliation on a square-tiled surface are closed. The *critical graph* Γ (*separatrix diagram*) is the union of all horizontal critical leaves. Vertices of Γ are represented by the conical points; the edges of Γ are formed by horizontal saddle connections (red in the picture).

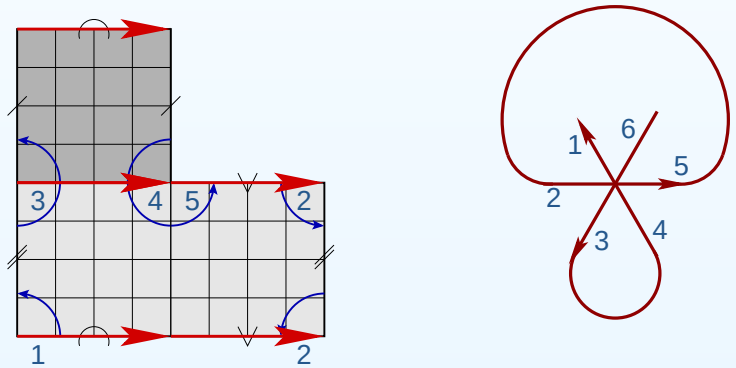

Let us construct the critical graph step-by-step. In our example the cone angle is 6π, so there are three outgoing separatrix rays and three incoming rays; they are alternated with respect to the natural cyclic order. Going around our conical singularity we can trace the order of appearance of horizontal rays and the way the prongs are joined into a graph. We see that the prong 3 is joined to prong 4; prong 5 is joined to prong 2,

Critical graph (separatrix diagram)

Note that all leaves of the horizontal (vertical) foliation on a square-tiled surface are closed. The *critical graph* Γ (*separatrix diagram*) is the union of all horizontal critical leaves. Vertices of Γ are represented by the conical points; the edges of Γ are formed by horizontal saddle connections (red in the picture).

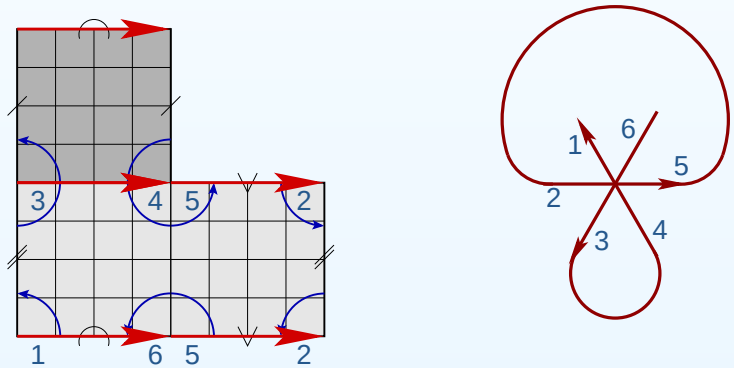

Let us construct the critical graph step-by-step. In our example the cone angle is 6π, so there are three outgoing separatrix rays and three incoming rays; they are alternated with respect to the natural cyclic order. Going around our conical singularity we can trace the order of appearance of horizontal rays and the way the prongs are joined into a graph. We see that the prong 3 is joined to prong 4; prong 5 is joined to prong 2,

Critical graph (separatrix diagram)

Note that all leaves of the horizontal (vertical) foliation on a square-tiled surface are closed. The *critical graph* Γ (*separatrix diagram*) is the union of all horizontal critical leaves. Vertices of Γ are represented by the conical points; the edges of Γ are formed by horizontal saddle connections (red in the picture).

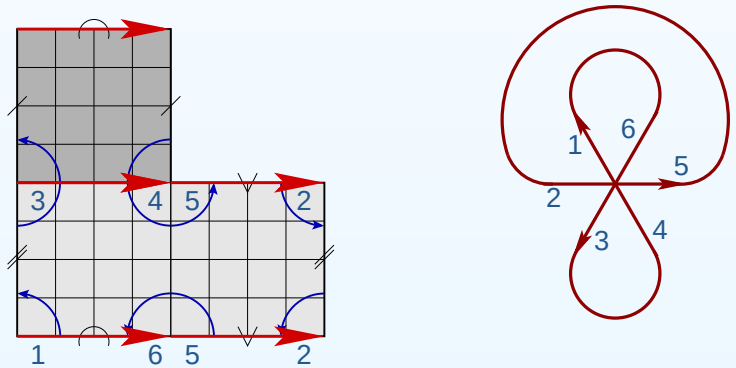

Let us construct the critical graph step-by-step. In our example the cone angle is 6π, so there are three outgoing separatrix rays and three incoming rays; they are alternated with respect to the natural cyclic order. Going around our conical singularity we can trace the order of appearance of horizontal rays and the way the prongs are joined into a graph. We see that the prong 3 is joined to prong 4; prong 5 is joined to prong 2, and prong 1 is joined to prong 6. The core of the critical graph is constructed.

Critical graph (separatrix diagram)

Note that all leaves of the horizontal (vertical) foliation on a square-tiled surface are closed. The *critical graph* Γ (*separatrix diagram*) is the union of all horizontal critical leaves. Vertices of Γ are represented by the conical points; the edges of Γ are formed by horizontal saddle connections (red in the picture).

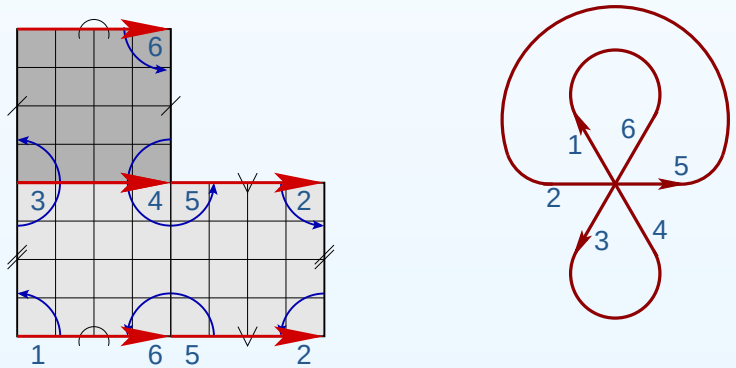

Let us construct the critical graph step-by-step. In our example the cone angle is 6π, so there are three outgoing separatrix rays and three incoming rays; they are alternated with respect to the natural cyclic order. Going around our conical singularity we can trace the order of appearance of horizontal rays and the way the prongs are joined into a graph. We see that the prong 3 is joined to prong 4; prong 5 is joined to prong 2, and prong 1 is joined to prong 6. The core of the critical graph is constructed.

Critical graph (separatrix diagram)

Note that all leaves of the horizontal (vertical) foliation on a square-tiled surface are closed. The *critical graph* Γ (*separatrix diagram*) is the union of all horizontal critical leaves. Vertices of Γ are represented by the conical points; the edges of Γ are formed by horizontal saddle connections (red in the picture).

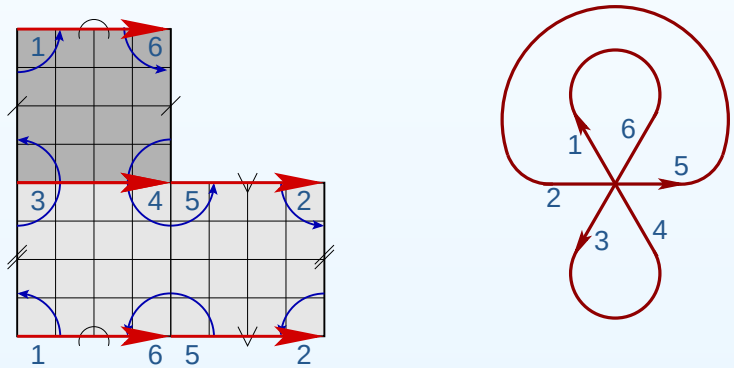

Let us construct the critical graph step-by-step. In our example the cone angle is 6π, so there are three outgoing separatrix rays and three incoming rays; they are alternated with respect to the natural cyclic order. Going around our conical singularity we can trace the order of appearance of horizontal rays and the way the prongs are joined into a graph. We see that the prong 3 is joined to prong 4; prong 5 is joined to prong 2, and prong 1 is joined to prong 6. The core of the critical graph is constructed.

Critical graph (separatrix diagram)

Note that all leaves of the horizontal (vertical) foliation on a square-tiled surface are closed. The *critical graph* Γ (*separatrix diagram*) is the union of all horizontal critical leaves. Vertices of Γ are represented by the conical points; the edges of Γ are formed by horizontal saddle connections (red in the picture).

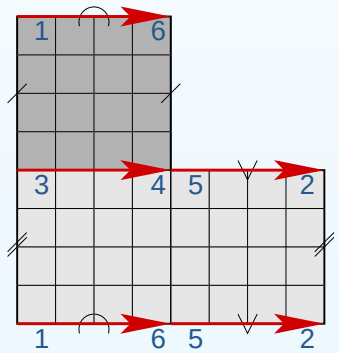

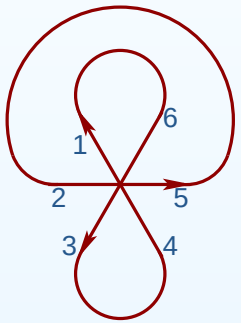

Critical graph (separatrix diagram)

Note that all leaves of the horizontal (vertical) foliation on a square-tiled surface are closed. The *critical graph* Γ (*separatrix diagram*) is the union of all horizontal critical leaves. Vertices of Γ are represented by the conical points; the edges of Γ are formed by horizontal saddle connections (red in the picture).

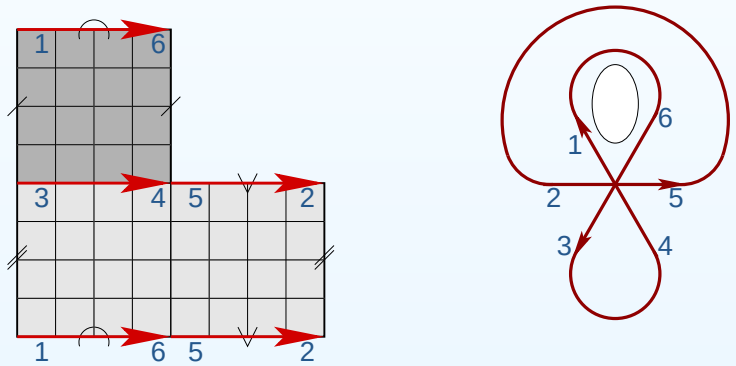

Our critical graph is embedded into a translation surface, so it carries an induced structure of a *ribbon graph* as if we would have oriented ribbons going along the edges with a well-defined cyclic order at every edge.

Critical graph (separatrix diagram)

Note that all leaves of the horizontal (vertical) foliation on a square-tiled surface are closed. The *critical graph* Γ (*separatrix diagram*) is the union of all horizontal critical leaves. Vertices of Γ are represented by the conical points; the edges of Γ are formed by horizontal saddle connections (red in the picture).

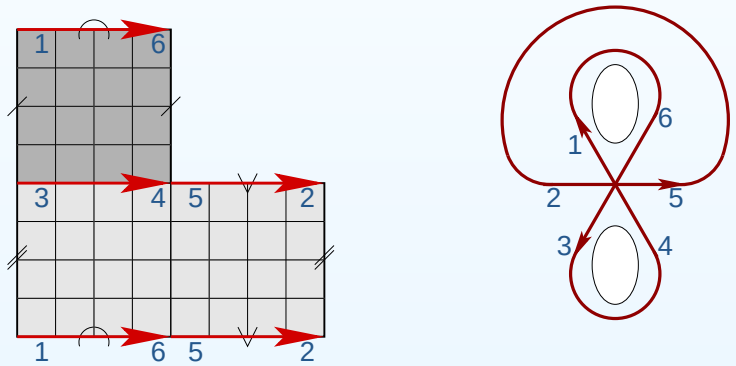

Our critical graph is embedded into a translation surface, so it carries an induced structure of a *ribbon graph* as if we would have oriented ribbons going along the edges with a well-defined cyclic order at every edge. We can reconstruct one-by-one the boundary components of the resulting ribbon graph.

Critical graph (separatrix diagram)

Note that all leaves of the horizontal (vertical) foliation on a square-tiled surface are closed. The *critical graph* Γ (*separatrix diagram*) is the union of all horizontal critical leaves. Vertices of Γ are represented by the conical points; the edges of Γ are formed by horizontal saddle connections (red in the picture).

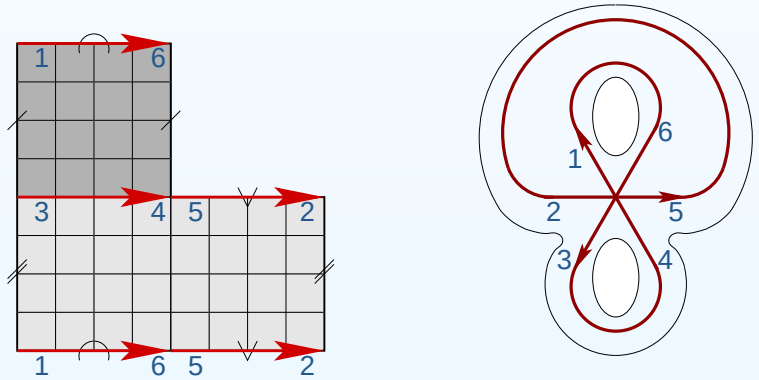

Our critical graph is embedded into a translation surface, so it carries an induced structure of a *ribbon graph* as if we would have oriented ribbons going along the edges with a well-defined cyclic order at every edge. We can reconstruct one-by-one the boundary components of the resulting ribbon graph.

Critical graph (separatrix diagram)

Note that all leaves of the horizontal (vertical) foliation on a square-tiled surface are closed. The *critical graph* Γ (*separatrix diagram*) is the union of all horizontal critical leaves. Vertices of Γ are represented by the conical points; the edges of Γ are formed by horizontal saddle connections (red in the picture).

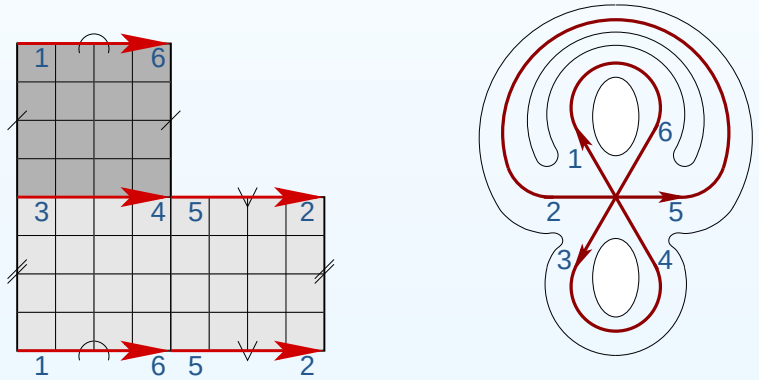

Our critical graph is embedded into a translation surface, so it carries an induced structure of a *ribbon graph* as if we would have oriented ribbons going along the edges with a well-defined cyclic order at every edge. We can reconstruct one-by-one the boundary components of the resulting ribbon graph.

Critical graph (separatrix diagram)

Note that all leaves of the horizontal (vertical) foliation on a square-tiled surface are closed. The *critical graph* Γ (*separatrix diagram*) is the union of all horizontal critical leaves. Vertices of Γ are represented by the conical points; the edges of Γ are formed by horizontal saddle connections (red in the picture).

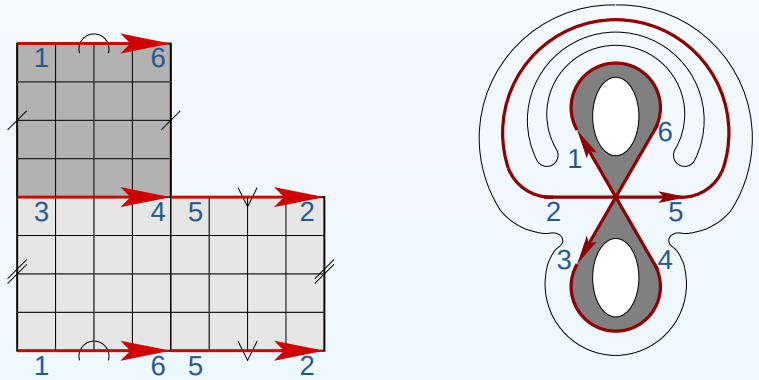

Our critical graph is embedded into a translation surface, so it carries an induced structure of a *ribbon graph* as if we would have oriented ribbons going along the edges with a well-defined cyclic order at every edge. We can reconstruct one-by-one the boundary components of the resulting ribbon graph. It remains to encode how the boundary components are organized into pairs, where each pair bounds a cylinder filled with parallel closed horizontal geodesics of equal length. We shade the first pair in dark and the second in light.

Critical graph (separatrix diagram)

Note that all leaves of the horizontal (vertical) foliation on a square-tiled surface are closed. The *critical graph* Γ (*separatrix diagram*) is the union of all horizontal critical leaves. Vertices of Γ are represented by the conical points; the edges of Γ are formed by horizontal saddle connections (red in the picture).

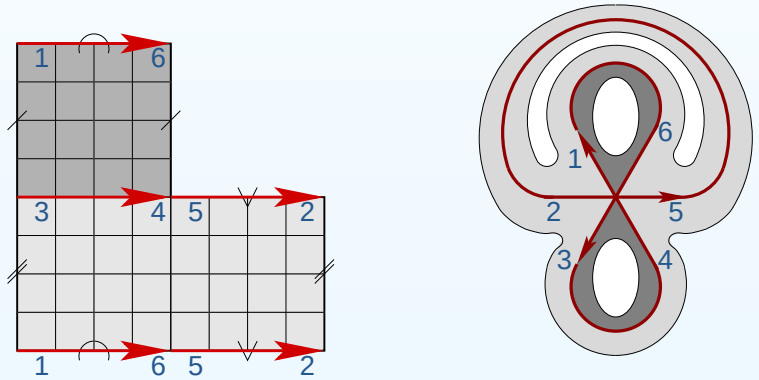

Our critical graph is embedded into a translation surface, so it carries an induced structure of a *ribbon graph* as if we would have oriented ribbons going along the edges with a well-defined cyclic order at every edge. We can reconstruct one-by-one the boundary components of the resulting ribbon graph. It remains to encode how the boundary components are organized into pairs, where each pair bounds a cylinder filled with parallel closed horizontal geodesics of equal length. We shade the first pair in dark and the second in light.

Critical graph (separatrix diagram)

Note that all leaves of the horizontal (vertical) foliation on a square-tiled surface are closed. The *critical graph* Γ (*separatrix diagram*) is the union of all horizontal critical leaves. Vertices of Γ are represented by the conical points; the edges of Γ are formed by horizontal saddle connections.

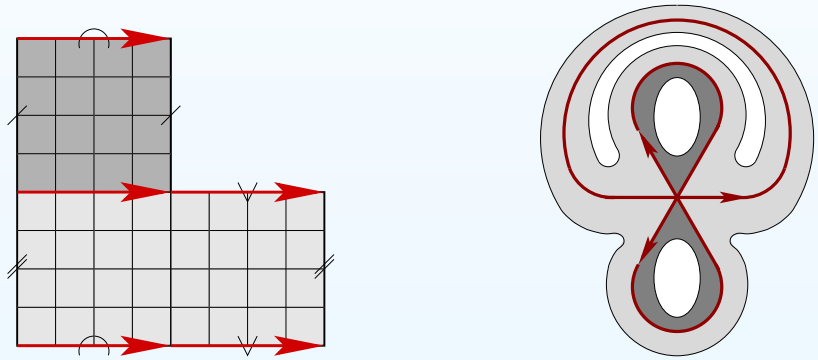

A *critical graph* Γ is an *oriented ribbon graph* endowed with the following structure:

1. The orientation of edges at any vertex is alternated with respect to the cyclic order of edges at this vertex.

2. The complement $S - \Gamma$ is a finite disjoint union of flat cylinders foliated by oriented circles. Thus, the set of boundary components of the ribbon graph is decomposed into pairs: to each pair of boundary components we glue a cylinder, and there is one positively oriented and one negatively oriented boundary component in each pair.

Realizable separatrix diagrams

Note, however, that not all ribbon graphs as above correspond to actual flat surfaces. A flat metric endows saddle connections with positive lengths ℓ_i. The left graph is realizable for any lengths ℓ_1, ℓ_2, ℓ_3. The middle one — only when $\ell_1 = \ell_3$. The rightmost one is never realizable: pairs of boundary components bounding the same cylinder have to have equal length, and we cannot find a pair for the component of length $\ell_1 + \ell_2 + \ell_3$.

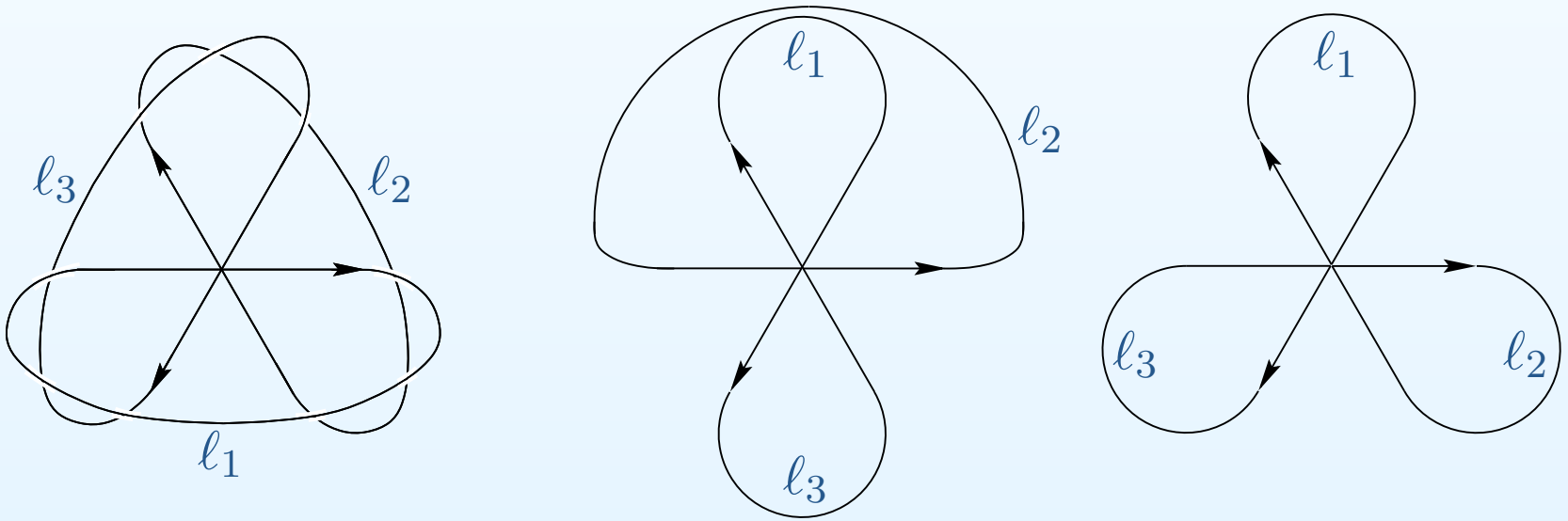

Lemma. *The set of all square-tiled surfaces sharing any realizable separatrix diagram provides a nontrivial contribution to the volume of the corresponding stratum.*

Volume computation for $\mathcal{H}(2)$: the 1-cylinder diagram

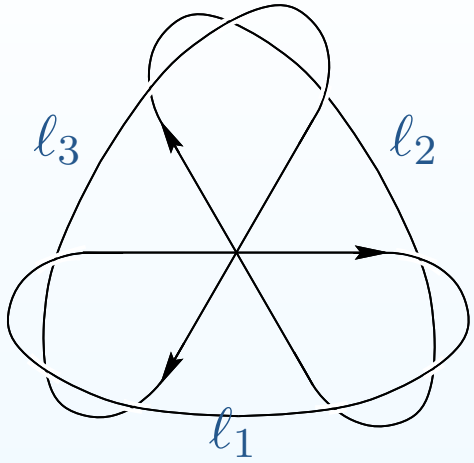

Single cylinder

$$\frac{1}{3} \sum_{\substack{\ell_1,\ell_2,\ell_3,h\in\mathbb{N} \\ (\ell_1+\ell_2+\ell_3)h\le N}} (\ell_1+\ell_2+\ell_3) \approx \frac{1}{3} \sum_{\substack{w,h\in\mathbb{N} \\ w\cdot h\le N}} w\cdot\frac{w^2}{2} = \frac{1}{6} \sum_{\substack{w,h\in\mathbb{N} \\ w\le \frac{N}{h}}} w^3$$

$$\approx \frac{1}{6} \sum_{h\in\mathbb{N}} \frac{1}{4}\cdot\left(\frac{N}{h}\right)^4 = \frac{N^4}{24}\cdot\sum_{h\in\mathbb{N}}\frac{1}{h^4}$$

$$= \frac{N^4}{24}\cdot\zeta(4) = \frac{N^4}{24}\cdot\frac{\pi^4}{90}\,.$$

Volume computation for $\mathcal{H}(2)$: the 2-cylinders diagram

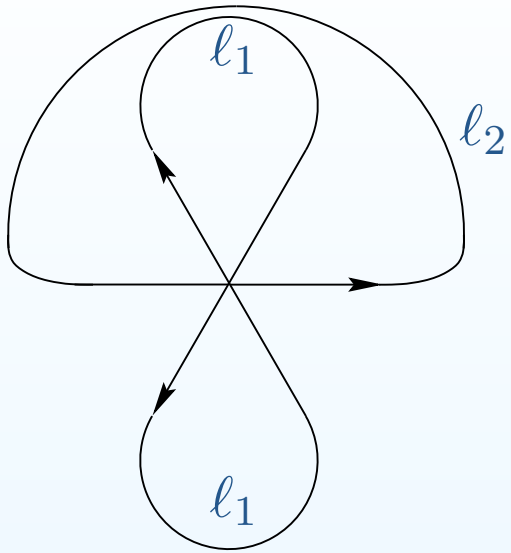

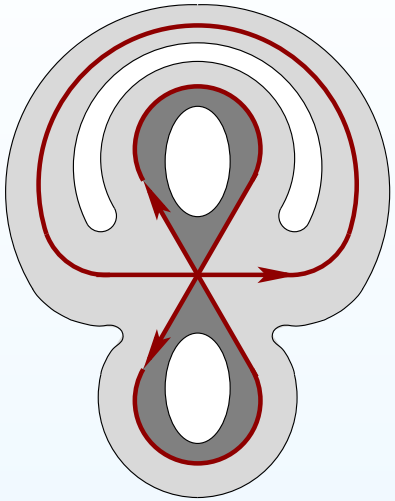

$$\sum_{\substack{\ell_1,\ell_2,h_1,h_2\in\mathbb{N}\\ \ell_1 h_1+(\ell_1+\ell_2)h_2\leq N}} \ell_1(\ell_1+\ell_2) = \sum_{\substack{\ell_1,\ell_2,h_1,h_2\in\mathbb{N}\\ \ell_1(h_1+h_2)+\ell_2 h_2\leq N}} (\ell_1^2+\ell_1\ell_2) =$$

$$= \sum_{h_1,h_2\in\mathbb{N}} \sum_{\substack{\ell_1,\ell_2\in\mathbb{N}\\ \frac{\ell_1(h_1+h_2)}{N}+\frac{\ell_2 h_2}{N}\leq 1}} (\ell_1^2+\ell_1\ell_2)\,.$$

Volume computation for $\mathcal{H}(2)$: the 2-cylinders diagram

For any fixed h_1, h_2 we can replace the sum with respect to ℓ_1, ℓ_2 by the integral. Let $x_1 := \ell_1 \cdot \dfrac{h_1 + h_2}{N}$ and $x_2 := \ell_2 \cdot \dfrac{h_2}{N}$ be the new variables, where h_1, h_2 are considered as parameters. After this change of variables our sums with respect to ℓ_1, ℓ_2 become the integral with respect to x_1, x_2, where we integrate over the simplex $\Delta = \{x_1 + x_2 \le 1 : x_1 \ge 0; x_2 \ge 0\}$:

$$\sum_{\substack{\ell_1,\ell_2 \in \mathbb{N} \\ \frac{\ell_1(h_1+h_2)}{N} + \frac{\ell_2 h_2}{N} \le 1}} (\ell_1^2 + \ell_1\ell_2) \approx$$

$$\approx \int_\Delta \left[\left(\frac{x_1 N}{h_1 + h_2} \right)^2 + \left(\frac{x_1 N}{h_1 + h_2} \right) \left(\frac{x_2 N}{h_2} \right) \right] \left(\frac{N}{h_1 + h_2} dx_1 \right) \left(\frac{N}{h_2} dx_2 \right) .$$

Multiple zeta-values

We will need the values of the sums

$$\zeta(s_1, s_2, \ldots, s_k) = \sum_{n_1,\ldots,n_k \geq 1} \frac{1}{n_1^{s_1}(n_1+n_2)^{s_2}\ldots(n_1+\cdots+n_k)^{s_k}}$$

at positive integers s_j, where $s_k \geq 2$. They are called *multiple zeta-values* and have beautiful properties, which recently attracted a lot of attention by Brown, Cartier, Deligne, Drinfeld, Écalle, Goncharov, Kontsevich, Zagier, to give only some names. We already used *zeta values* as

$$\zeta(2) = \frac{\pi^2}{6}; \qquad \zeta(4) = \frac{\pi^4}{90}; \qquad \zeta(2n) = \frac{p}{q} \cdot \pi^{2n}, \quad \text{where } p, q \in \mathbb{N}\,.$$

Multiple zeta-values

We will need the values of the sums

$$\zeta(s_1, s_2, \ldots, s_k) = \sum_{n_1,\ldots,n_k \geq 1} \frac{1}{n_1^{s_1}(n_1+n_2)^{s_2}\ldots(n_1+\cdots+n_k)^{s_k}}$$

at positive integers s_j, where $s_k \geq 2$. They are called *multiple zeta-values* and have beautiful properties, which recently attracted a lot of attention by Brown, Cartier, Deligne, Drinfeld, Écalle, Goncharov, Kontsevich, Zagier, to give only some names. We already used *zeta values* as

$$\zeta(2) = \frac{\pi^2}{6}; \qquad \zeta(4) = \frac{\pi^4}{90}; \qquad \zeta(2n) = \frac{p}{q} \cdot \pi^{2n}, \quad \text{where } p, q \in \mathbb{N}\,.$$

Conjecturally $\pi, \zeta(3), \zeta(5), \ldots$ are algebraically independent over $\mathbb{Q}$. However, multiple zeta values satisfy numerous relations, some of them were discovered already by Euler, for example

$$\zeta(1,3) = \frac{1}{4}\,\zeta(4); \qquad \zeta(2,2) = \frac{3}{4}\,\zeta(4)\,.$$

Volume computation for $\mathcal{H}(2)$: the 2-cylinders diagram

$$\sum_{h_1,h_2} \int_\Delta \left[\left(\frac{x_1 N}{h_1+h_2} \right)^2 + \left(\frac{x_1 N}{h_1+h_2} \right) \left(\frac{x_2 N}{h_2} \right) \right] \left(\frac{N}{h_1+h_2} dx_1 \right) \left(\frac{N}{h_2} dx_2 \right)$$

$$= N^4 \left[\int_\Delta x_1^2 \, dx_1 dx_2 \cdot \sum_{h_1,h_2 \in \mathbb{N}} \frac{1}{h_2 (h_1+h_2)^3} \right.$$

$$\left. + \int_\Delta x_1 x_2 \, dx_1 dx_2 \cdot \sum_{h_1,h_2 \in \mathbb{N}} \frac{1}{h_2^2 (h_1+h_2)^2} \right]$$

$$= \frac{N^4}{24} \big[2 \cdot \zeta(1,3) + \zeta(2,2) \big] = \frac{N^4}{24} \left[2 \cdot \frac{\zeta(4)}{4} + \frac{3\zeta(4)}{4} \right]$$

$$= \frac{N^4}{24} \cdot \frac{5}{4} \cdot \frac{\pi^4}{90}.$$

where we used the identities $\zeta(1,3) = \frac{1}{4}\,\zeta(4), \quad \zeta(2,2) = \frac{3}{4}\,\zeta(4)$ and the values $\int_\Delta x_1^2 \, dx_1 dx_2 = 2 \int_\Delta x_1 x_2 \, dx_1 dx_2 = 2 \cdot \frac{1}{4!}$.

Volume computation for $\mathcal{H}(2)$: summary

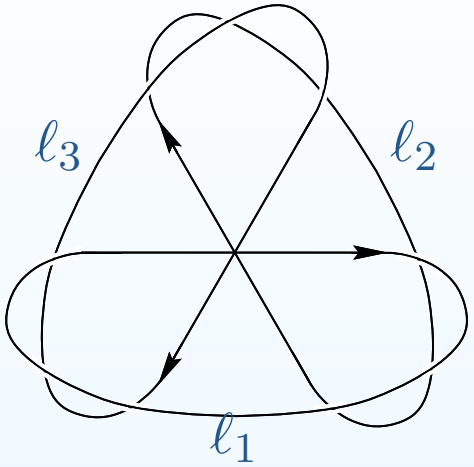

$$\frac{1}{3} \sum_{\substack{\ell_1,\ell_2,\ell_3,h\in\mathbb{N} \\ (\ell_1+\ell_2+\ell_3)h\le N}} (\ell_1+\ell_2+\ell_3) \approx \frac{N^4}{24}\cdot\zeta(4)$$

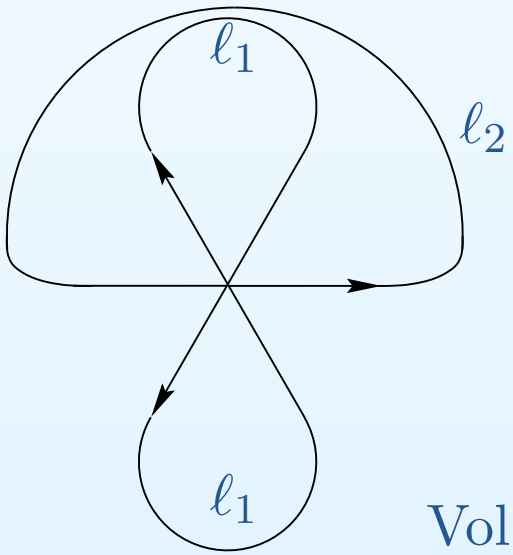

$$\sum_{\substack{\ell_1,\ell_2,h_1,h_2 \\ \ell_1 h_1+(\ell_1+\ell_2)h_2\le N}} \ell_1(\ell_1+\ell_2)$$

$$= \frac{N^4}{24}\big[2\cdot\zeta(1,3)+\zeta(2,2)\big] = \frac{N^4}{24}\cdot\frac{5}{4}\cdot\zeta(4)$$

$$\mathrm{Vol}(\mathcal{H}_1(2)) = \lim_{N\to\infty}\frac{2\cdot 4}{N^4}\cdot(\text{Number of surfaces}) = \frac{\pi^4}{120}$$

Contributions $\mathrm{Vol}_k\,\mathcal{H}(3,1)$ of k-cylinder surfaces to $\mathrm{Vol}\,\mathcal{H}(3,1)$

$$\mathrm{Vol}_1\mathcal{H}(3,1) = \frac{\zeta(7)}{15}$$

$$\mathrm{Vol}_2\mathcal{H}(3,1) = \frac{55\,\zeta(1,6) + 29\,\zeta(2,5) + 15\,\zeta(3,4) + 8\,\zeta(4,3) + 4\,\zeta(5,2)}{45}$$

$$\begin{aligned}\mathrm{Vol}_3\mathcal{H}(3,1) = \frac{1}{90}\Big(&12\,\zeta(6) - 12\,\zeta(7) + 48\,\zeta(4)\,\zeta(1,2) + 48\,\zeta(3)\,\zeta(1,3)\\ &+ 24\,\zeta(2)\,\zeta(1,4) + 6\,\zeta(1,5) - 250\,\zeta(1,6) - 6\,\zeta(3)\,\zeta(2,2)\\ &- 5\,\zeta(2)\,\zeta(2,3) + 6\,\zeta(2,4) - 52\,\zeta(2,5) + 6\,\zeta(3,3) - 82\,\zeta(3,4)\\ &+ 6\,\zeta(4,2) - 54\,\zeta(4,3) + 6\,\zeta(5,2) + 120\,\zeta(1,1,5) - 30\,\zeta(1,2,4)\\ &- 120\,\zeta(1,3,3) - 120\,\zeta(1,4,2) - 54\,\zeta(2,1,4) - 34\,\zeta(2,2,3)\\ &- 29\,\zeta(2,3,2) - 88\,\zeta(3,1,3) - 34\,\zeta(3,2,2) - 48\,\zeta(4,1,2)\Big)\end{aligned}$$

$$\mathrm{Vol}_4\mathcal{H}(3,1) = \frac{2\zeta(2)}{45}\Big(\zeta(4) - \zeta(5) + \zeta(1,3) + \zeta(2,2) - \zeta(2,3) - \zeta(3,2)\Big)\,.$$

After simplification

Multiple zeta values satisfy numerous relations. After simplification (which is now accessible through a SAGE package) we get

$$\begin{aligned}
&\mathrm{Vol}_1\,\mathcal{H}(3,1) = 1/15\cdot\zeta(7)\\
&\mathrm{Vol}_2\,\mathcal{H}(3,1) = -7/135\cdot\zeta(1,6) + 1/135\cdot\zeta(2,5) + 23/135\cdot\zeta(7)\\
&\mathrm{Vol}_3\,\mathcal{H}(3,1) = -2/15\cdot\zeta(1,6) - 2/45\cdot\zeta(2,5) + 1/5\cdot\zeta(6) - 4/45\cdot\zeta(7)\\
&\mathrm{Vol}_4(\mathcal{H}(3,1) = 5/27\cdot\zeta(1,6) + 1/27\cdot\zeta(2,5) + 7/45\cdot\zeta(6) - 4/27\cdot\zeta(7)
\end{aligned}$$

Conjecturally, multiple zeta values involved in these simplified expressions are linearly independent over rational numbers. However, the total contribution is a rational multiple of π^{2g} in accordance with the general result by A. Eskin and A. Okounkov, 2001:

$$\mathrm{Vol}\,\mathcal{H}(3,1) = \mathrm{Vol}_1\,\mathcal{H}(3,1) + \cdots + \mathrm{Vol}_4\,\mathcal{H}(3,1) = \frac{16}{42525}\pi^6$$

Volumes of some low-dimensional strata

$$
\begin{aligned}
\mathrm{Vol}(\mathcal{H}_1(\emptyset)) &= 2\cdot\zeta(2) &&= \frac{1}{3}\cdot\pi^2\\
\mathrm{Vol}(\mathcal{H}_1(2)) &= \frac{2}{3!}\cdot\frac{9}{4}\cdot\zeta(4) &&= \frac{1}{120}\cdot\pi^4\\
\mathrm{Vol}(\mathcal{H}_1(1,1)) &= \frac{1}{4!}\cdot 4\cdot\zeta(4) &&= \frac{1}{135}\cdot\pi^4\\
\mathrm{Vol}(\mathcal{H}_1^{hyp}(4)) &= \frac{2}{5!}\cdot\frac{135}{16}\cdot\zeta(6) &&= \frac{1}{6720}\cdot\pi^6\\
\mathrm{Vol}(\mathcal{H}_1^{odd}(4)) &= \frac{2}{5!}\cdot\frac{70}{3}\cdot\zeta(6) &&= \frac{1}{2430}\cdot\pi^6\\
\mathrm{Vol}(\mathcal{H}_1(1,3)) &= \frac{2}{6!}\cdot 128\cdot\zeta(6) &&= \frac{16}{42525}\cdot\pi^6\\
\mathrm{Vol}(\mathcal{H}_1^{hyp}(6)) &= \frac{2}{7!}\cdot\frac{2625}{64}\cdot\zeta(8) &&= \frac{1}{580608}\cdot\pi^8
\end{aligned}
$$

Volumes through multiple zeta values

Conjecture. *Prove that for any connected component of any stratum the contribution to the Masur–Veech volume coming from square-tiled having exatly k horizontal cylinders is a linear combination with rational coefficients of multiple zeta values.*

Stronger Conjecture. *Prove the that contribution to the Masur–Veech volume coming from square-tiled corresponding to any fixed separatrix diagram is a linear combination with rational coefficients of multiple zeta values.*

The latter statement is elementary for 1-cylinder separatrix diagrams, simple for 2-cylinder diagrams. It is already a nontrivial theorem (proved by B. Allombert and V. Delecroix) for 3-cylinder diagrams.

Homework assignment

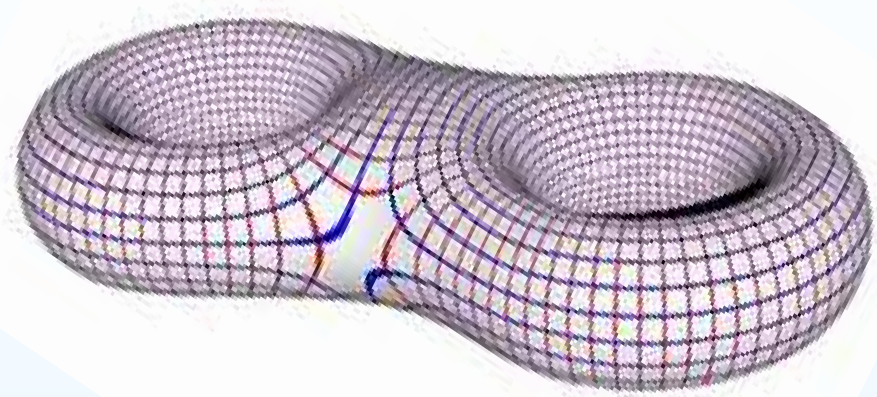

Picture created by Jian Jiang

Questions.

- *To what stratum belongs this square-tiled surface?*
- *Find all realizabe separatrix diagrams for this stratum.*
- *To which of the found diagrams corresponds the square-tiled surface from the picture?*

Outline of approaches to evaluation of Masur–Veech volumes

Masur–Veech volumes of strata of Abeliand differentials: a historical retrospective

- Around 1998. Masur–Veech volumes of several low-dimensional strata of Abelian differentials were evaluated by M. Kontsevich and A. Zorich through straightforward count of square-tiled surfaces.

- Around 2001. A. Eskin and A. Okounkov found a much more efficient approach based on quasimodularity of an associated generating function. A. Eskin wrote a computer code giving volumes of all strata in genera at most 10 and of some strata in genera up to 200.

- 2020. D. Chen, M. Möller, A. Sauvaget and D. Zagier obtained very important advances based on recent BCGGM smooth compactification of the moduli space of Abelian differentials. They developed intersection theory of relevant moduli spaces and found a recursive formula for volumes.

- 2018–2020. D. Chen–M. Möller–A. Sauvaget–D. Zagier and independently A. Aggarwal obtained spectacular results on large genus asymptotics of Masur–Veech volumes uniform for all strata stratum of Abelian differentials proving a conjecture by A. Eskin and of A. Zorich based on their numerical experiments from 2003.

Masur–Veech volumes of strata of quadratic differentials: a brief historical retrospective

The knowledge of Masur–Veech volumes $\mathrm{Vol}\, \mathcal{Q}_1(d_1, \dots, d_k)$ of strata of *quadratic* differentials is still limited.

• Around 1998-2000. Masur–Veech volumes of several low-dimensional strata of quadratic differentials were evaluated by A. Zorich through straightforward count of square-tiled surfaces.

• 2001. A. Eskin and A. Okounkov found a much more efficient approach based on quasimodularity of the generating function counting *pillowcase covers*. However, the resulting expressions contain huge tables of characters of the symmetric group, which makes the computation inefficient. The algorithm is more involved than for Abelian differentials.

• 2016. The algorithm of A. Eskin and A. Okounkov was implemented by E. Goujard. She wrote a code and computed volumes of all strata up to dimension 12.

Masur–Veech volumes of strata of quadratic differentials: a brief historical retrospective

- 2016. J. Athreya–A. Eskin–A. Zorich obtained a close expression (conjectured by M. Kontsevich) for the Masur–Veech volume of any stratum in genus zero through the formula of A. Eskin–M. Kontsevich–A. Zorich for the sum of Lyapunov exponents combined with some combinatorial considerations.
- 2019. V. Delecroix–E. Goujard–P. Zograf–A. Zorich computed volumes of the principal strata (the ones containing only simple zeroes and poles) in terms of Witten–Kontsevich correlators.
- 2019. D. Chen–M. Möller–A. Sauvaget expressed volumes of the principal strata in terms of certain Hodge integrals.
- 2019. J. Andersen–G. Borot–S. Charbonnier–V. Delecroix–A. Giacchetto–D. Lewanski–C. Wheeler used the DGZZ-formula to compute volumes through topological recursion.
- 2020. M. Kazarian and independently Di Yang–D. Zagier–Y. Zhang developed efficient recursion for the Hodge integrals involved in the CMS-formula.
- 2021. A. Aggarwal derived the large genus asymptotics for the volumes of principal strata conjectured by V. Delecroix–E. Goujard–P. Zograf–A. Zorich.

Open problem: volumes of strata of quadratic differentials

Let $\boldsymbol{d} = (d_1, \dots, d_n)$ be an unordered partition of a positive integer number $4g-4$ divisible by 4 into a sum $|\boldsymbol{d}| = d_1 + \dots + d_n = 4g-4$, where $d_i \in \{-1, 0, 1, 2, \dots\}$ for $i = 1, \dots, n$. Denote by $\hat{\Pi}_{4g-4}$ the set of those partitions as above, which satisfy the additional requirement that the number of entries $d_i = -1$ in $\boldsymbol{d}$ is at most $\log(g)$.

Open problem. *Find the Masur–Veech volume of strata $\mathcal{Q}(d_1, \dots, d_n)$ of meromorphic quadratic differentials with at most simple poles when at least one od d_i is even. Prove the following conjectural asymptotic formula (currently proved by A. Aggarwal only for the principal stratum): for any $\boldsymbol{d} \in \hat{\Pi}_{4g-4}$ one has*

$$\operatorname{Vol} \mathcal{Q}(d_1, \dots, d_n) = \frac{4}{\pi} \cdot \prod_{i=1}^{n} \frac{2^{d_i+2}}{d_i+2} \cdot \big(1 + \varepsilon_1(\boldsymbol{d})\big)\,,$$

where

$$\lim_{g\to\infty} \max_{\boldsymbol{d}\in\hat{\Pi}_{4g-4}} |\varepsilon_1(\boldsymbol{d})| = 0\,.$$

For strata of dimension up to 12 the volumes are found by E. Goujard using Eskin–Okounkov algorithm.


2 ARR.T
RUE DES
PETITS CARREAUX